Biomaterials 271 (2021) 120750

Contents lists available at ScienceDirect

Biomaterials

journal homepage: www.elsevier.com/locate/biomaterials

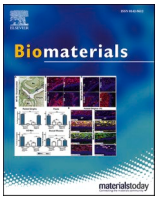

Stable oxime-crosslinked hyaluronan-based hydrogel as a biomimetic vitreous substitute

Alexander E.G. Baker [a,b], Hong Cui [a], Brian G. Ballios [e], Sonja Ing [b], Peng Yan [c], Joe Wolfer [d], Thomas Wright [c,e], Mickael Dang [a], Nicola Y. Gan [f], Michael J. Cooke [b], Arturo Ortín-Martínez [g], Valerie A. Wallace [e,g,h], Derek van der Kooy [i,j], Robert Devenyi [e,g,k], Molly S. Shoichet [a,b,j,*]

[a] Department of Chemical Engineering and Applied Chemistry, University of Toronto, 200 College St, Toronto, ON, M5S 3E5, Canada
[b] Institute of Biomedical Engineering, University of Toronto, 160 College St, Toronto, ON, M5S 3E1, Canada
[c] Kensington Eye Institute, 340 College St, Toronto, ON, M5T 3A9, Canada
[d] Toronto Animal Eye Clinic, 150 Norseman St, Etobicoke, ON, M8Z 2R4, Canada
[e] Department of Ophthalmology and Vision Sciences, University of Toronto, 340 College St, Toronto, ON, L0J 1C0, Canada
[f] Department of Ophthalmology, Tock Seng Hospital, National Healthcare Group Eye Institute, 11 Jln Tan Tock Seng, 308433, Singapore
[g] Donald K Johnson Eye Institute, Krembil Research Institute, University Health Network, 399 Bathurst St, Toronto, ON, M5T 2S8, Canada
[h] Department of Laboratory Medicine and Pathobiology, University of Toronto, 1 King's College Circle, ON, M5S 1A8, Canada
[i] Department of Molecular Genetics, University of Toronto, 1 King's College Circle, ON, M5S 1A8, Canada
[j] Institute of Medical Sciences, University of Toronto, 1 King's College Circle, ON, M5S 1A8, Canada
[k] Toronto Western Hospital, 399 Bathurst St, Room 6 E W 438, Toronto, ON, M5T 2S8, Canada

ARTICLE INFO

Keywords:
Hydrogel
Retinal tamponade
Retinal detachment
Vitreous substitute
Hyaluronan

ABSTRACT

Vitreous substitutes are clinically used to maintain retinal apposition and preserve retinal function; yet the most used substitutes are gases and oils which have disadvantages including strict face-down positioning post-surgery and the need for subsequent surgical removal, respectively. We have engineered a vitreous substitute comprised of a novel hyaluronan-oxime crosslinked hydrogel. Hyaluronan, which is naturally abundant in the vitreous of the eye, is chemically modified to crosslink with poly(ethylene glycol)-tetraoxyamine via oxime chemistry to produce a vitreous substitute that has similar physical properties to the native vitreous including refractive index, density and transparency. The oxime hydrogel is cytocompatible in vitro with photoreceptors from mouse retinal explants and biocompatible in rabbit eyes as determined by histology of the inner nuclear layer and photoreceptors in the outer nuclear layer. The ocular pressure in the rabbit eyes was consistent over 56 d, demonstrating limited to no swelling. Our vitreous substitute was stable in vivo over 28 d after which it began to degrade, with approximately 50% loss by day 56. We confirmed that the implanted hydrogel did not impact retina function using electroretinography over 90 days versus eyes injected with balanced saline solution. This new oxime hydrogel provides a significant improvement over the status quo as a vitreous substitute.

1. Introduction

The vitreous humor is a clear gelatinous substance composed of hyaluronan (HA) and collagen (types II, V/XI, and IX) and occupies the space between the lens and the retina [1–3]. Vitreoretinal surgeons frequently remove the vitreous to repair the retina or to perform subretinal injections then replace it with either a gas, such as sulfur hexafluoride (SF_6) or perfluoropropane (C_3F_8), or a non-biodegradable liquid, such as perfluorocarbons or silicone oil. Unfortunately, both options are sub-optimal for patients resulting in blurred vision for several weeks, face-down posturing for several days (for gasses) and often a second surgery (for silicone oils) [4,5]. One promising solution to rapidly restore patient vision are hydrogel vitreous substitutes. This relies on advances in biomaterials and crosslinking strategies devised to match the physical properties of the native vitreous, be biocompatible, that are stable, and bioresorbable; therefore, surgical resection can be avoided [6]. Despite promising studies reporting polymeric vitreous substitutes, they are each limited in utility due to swelling characteristics, a lack of tunable gelation rates and limited quantitative data on in vivo stability [7–9]. An ideal hydrogel vitreous substitute will

* Corresponding author. Department of Chemical Engineering and Applied Chemistry, University of Toronto, 200 College St, Toronto, ON, M5S 3E5, Canada.
E-mail address: molly.shoichet@utoronto.ca (M.S. Shoichet).

https://doi.org/10.1016/j.biomaterials.2021.120750
Received 28 October 2020; Received in revised form 26 February 2021; Accepted 2 March 2021
Available online 4 March 2021

tamponade the retina for 4–6 weeks while also address the above criteria [10].

Synthetic hydrogels, formed by in situ thermogelation or chemical crosslinking, have been investigated as vitreous substitutes but have narrow gelation tunability, often forming a gel before injection [8,11]. For example, poly(methacrylamide), poly(methacrylate), poly(ethylene glycol) (PEG) and poly(vinyl alcohol) (PVA) have all been formulated as hydrogels to treat retinal detachment [12–14]; yet, the polymers have been crosslinked with cytotoxic small molecules, require potentially harmful UV light, or use functional groups that are unstable in air [15,16]. Some patients treated with MIRAgel, poly(methylacrylate-co-2-hydroxyethyl acrylate), developed complications attributed to hydrolysis and hydrogel swelling that required removal [17–19]. Poly(alkylimide) hydrogels were found to induce severe retinal damage in pigmented rabbits [20]. Interestingly, a thiol-maleimide chemically crosslinked PEG hydrogel demonstrated excellent in vivo stability for up to 410 d [9]; however, storage is limited and problematic since thiol groups can oxidize quickly in air to form disulfides and are then unreactive while maleimides themselves hydrolyse in solution [21,22]. This limitation of thiol group oxidation is problematic for a PEG crosslinked PVA hydrogel (developed by Pykus) that requires a thiol-acrylate reaction. While the hydrogel itself is degradable via ester linkages and is compatible in rabbit eyes [23], PEG-thiols will form disulfide bonds that prevent crosslinking and PVA has been reported to cause vacuolations of the inner retina in macaques [24].

Natural biopolymers, such as HA (HYVISC®) and collagen, have been studied as vitreous substitutes, but had limited (if any) clinical efficacy or stability, requiring chemical crosslinking to avoid clearance

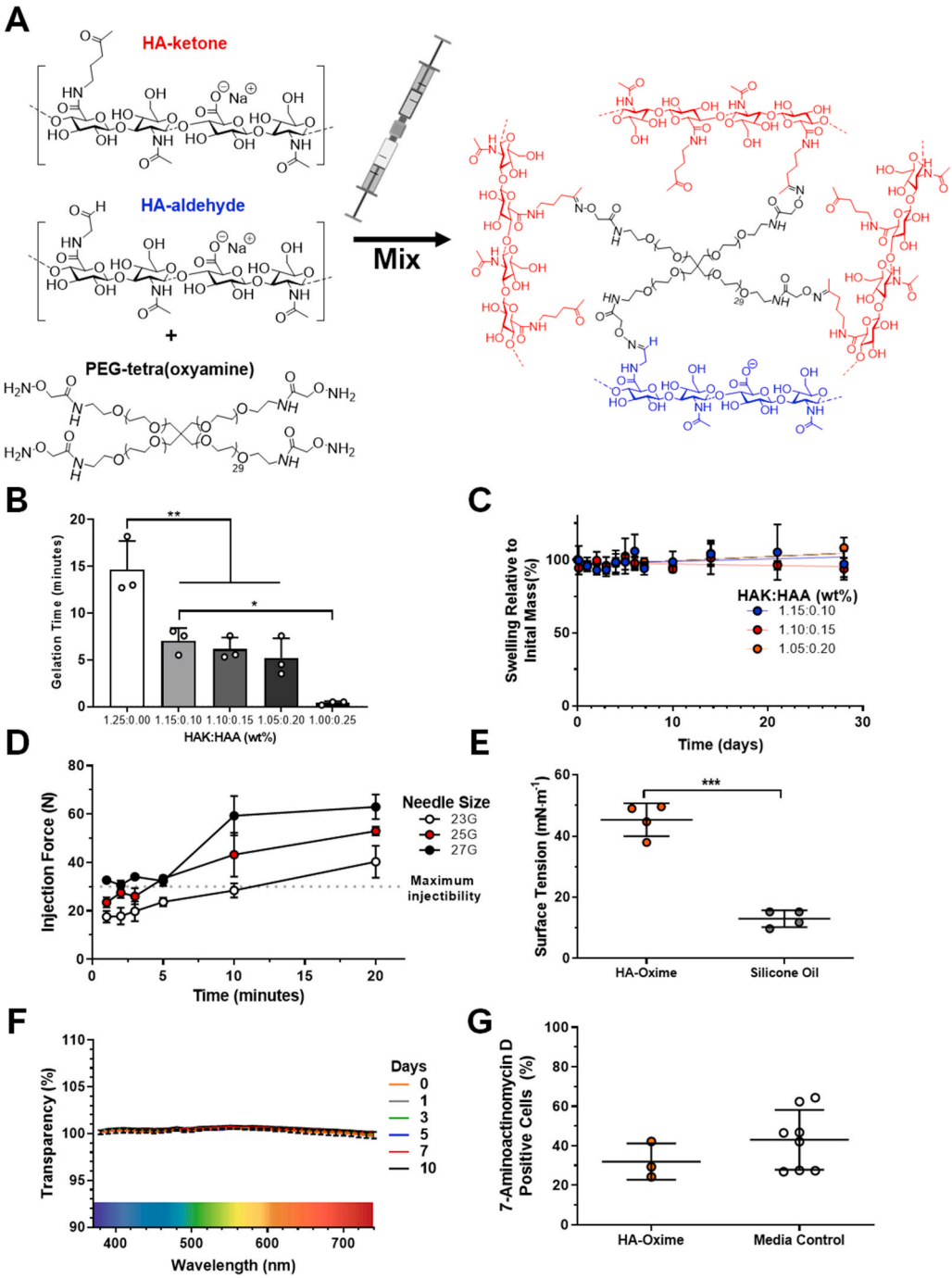

Fig. 1. Characterization of the HA-oxime vitreous substitute hydrogel. (A) HA-oxime hydrogel is synthesized by mixing hyaluronan-ketone (HAK) and hyaluronan-aldehyde (HAA) with poly(ethylene glycol)-tetraoxyamine (PEG OA_4), in separate syringes with a coupler, to form a crosslinked gel. (B) Gelation time for HA-oxime is faster with increased weight percent of HAA measured by rheology (n = 3, mean ± standard deviation, *p < 0.05, **p < 0.01 one-way ANOVA Tukey's post hoc test). (C) Swelling of HA-oxime hydrogels over 28 d in balanced saline solution is minimal as measured by change in mass relative to initial hydrogel mass (1.15:0.10; 1.10:0.15; 1.05:0.20, HAK:HAA, wt%/wt% n = 3–5, mean ± standard deviation). (D) HA-oxime hydrogel (1.05:0.20 HAK:HAA, wt%/wt%) is injectable by hand though a 23 gauge needle over 10 min and a 25 gauge needle over 5 min (n = 3, mean ± standard deviation). (E) Surface tension of HA-oxime hydrogel (1.05:0.20 HAK:HAA, wt%/wt%) is significantly higher than silicone oil (n = 4, mean ± standard deviation ***p < 0.001 Student's t-test). (F) HA-oxime hydrogels retain high transparency over 10 d with in vitro hyaluronidase treatment measured between λ = 380–740 nm (n = 3, mean ± standard deviation). (G) Viability of mouse retinal explants is unchanged in the presence or absence of HA-oxime hydrogels: percent of 7-aminoactinomycin D (i.e., dead or damaged cells) photoreceptors from mouse retinal explants after 24 h of culture, as measured by flow cytometry (n = 3 for HA-oxime; n = 8 for media control, mean ± standard deviation, not statistically significant (ns), p = 0.275 Student's t-test).

(Table S1, Supporting Information) [15,25–33]. Yet, care must be taken in the crosslinking chemistry used as a hydrazone-crosslinked HA vitreous substitute (Vitargus ABV-1701) [34] resulted in increased ocular pressure in 3 of 11 patients due to the uncontrolled and rapid swelling initiated by the hydrolysis of the hydrazone bonds, causing glaucoma in these patients and then subsequent medical intervention [35]. Healaflow™, an HA gel crosslinked with 1,4-butanediol diglycidyl ether was tolerated when implanted in the vitreous cavity of pigmented rabbits, but lasted only 14 d, which is sub-optimal for healing [31]. Self-assembled peptides, such as the PanaceaGel (SPG-178), are simple one component systems that are biocompatible in rabbit eyes; however, it is unclear whether they can be degraded by intravitreal matrix metalloproteinases [7,36].

The oxime reaction between either an aldehyde or ketone and an oxyamine is a versatile strategy to prepare hydrogels [37]. Hyaluronan-oxime hydrogels traditionally use HA-aldehyde, which reacts quickly, making them difficult to use as injectable hydrogels [38]. The kinetics of the oxime reaction can be altered by changing the pH, inclusion of salts, catalytic amine buffers, or by using a ketone group instead of an aldehyde [39–41]. Due to the sensitivity of the eye to pH and ionic strength, which could also affect the ocular pressure [42–44], we specifically designed our hydrogel to be comprised of hyaluronan-ketone and hyaluronan-aldehyde. We engineered a new oxime hydrogel vitreous substitute using a click-crosslinked system, comprised of HA-aldehyde, HA-ketone and PEG-oxyamine. The oxime click chemistry requires no catalysts or small molecules, generates hydrolytically stable linkages, thereby preventing swelling, and has tunable gelation rates. Gelation is controlled by the concentration of the functional groups and can be tuned from minutes to hours after mixing and before injection into the eye (Fig. 1A). We recognized the need to have an injectable solution with rapid gelation given the turnover of aqueous humor in both rabbits (2.25 μL min^{-1}), which we study herein, and humans (2.08 μL min^{-1}), our ultimate application [45–47]. This is the first reported use of an oxime hydrogel designed to replace the vitreous and tested in the eye. We selected the rabbit model given the extensive use to evaluate ophthalmic therapies [48,49]. We characterized the physical properties of this new hydrogel, evaluated it in vitro with primary photoreceptors, and characterized its long-term (56 d) stability and biocompatibility in vivo in New Zealand White rabbits. We monitored the in vivo stability of the hydrogel by measuring its mass and the depletion of fluorescence over time. The degradation of chemically crosslinked hydrogels cannot be analyzed by those methods typically used to characterize the degradation of linear polymers, such as by loss of molar mass (e.g., by gel permeation chromatography or NMR) due to the limited dissolution of crosslinked polymers. The hydrogel was confirmed to facilitate retina function and maintained the retina architecture in Dutch-Belted pigmented rabbits over 90 days using through electroretinography (ERG) measurements and optical coherence tomography (OCT), respectively. Together these studies establish crosslinked HA-oxime as an excellent choice for a vitreous substitute for the treatment of retinal detachment.

2. Methods

2.1. Materials

All chemical reagents were used directly as provided by the suppliers unless otherwise stated. The following reagents were purchased from Sigma-Aldrich: *N,N*-diisopropylethylamine, (boc-aminooxy)acetic acid, phosphate buffered saline. Sodium hyaluronate M_w 242 kDa (Lifecore Biomedical), poly(ethylene glycol)-tetra(amine) average M_n 5250 Da (Jenkem Technology), 4-(4,6-dimethoxy-1,3,5-triazin-2-yl)-4-methylmorpholinium chloride (Tokyo Chemical Industry), AlexaFluor™-647 hydrazide (Thermo Fisher Scientific), *N,N′*-diisopropylcarbodiimide (Tokyo Chemical Industry), methyl cellulose dialyzis membranes of 1000 Da and 12–14 kDa cut-off (Spectrum Laboratories), Hoechst 33342 (Cell Signaling Technology), calcein AM (Biotium Inc.) ethidium homodimer (Biotium Inc.), alumina oxide gamma-phase (Alfa Aesar) 23 GA TotalPlus® Vitrectomy Pak (Alcon), Endotoxin test kit (GenScript, catalogue number l00350), balanced salt solution (Alcon), Tobradex (Alcon), Tear-Gel Ophthalmic Liquid Gel (Novartis), All solvents were purchased from Caledon.

2.2. Synthesis of vitreous gel components

Ketone-modified hyaluronan (HAK) was synthesized as previously reported [50]. Briefly, sodium hyaluronate (1.00 g, 242 kDa) was dissolved in 2-(*N*-morpholino)ethanesulfonic acid (MES) buffer (100 mL, 0.1 M in water, pH 6.6) and stirred with DMTMM (1.21 g, 4.36 mmol). After 30 min, 3-(2-methyl-1,3-dioxolan-2-yl)propan-1-amine (0.36 g, 2.5 mmol) was added dropwise and stirred for 48 h. The solution was dialyzed in 0.1 M NaCl using methyl cellulose dialyzis membrane (12–14 kDa molecular weight cut-off) for 48 h followed by distilled water for 24 h. The purified solution was lyophilized and was analyzed by ^{1}H NMR in deuterium oxide to determine ketal substitution (40–45%). Ketal-substituted hyaluronan (HA-ketal) was dissolved in distilled water (1.0% w/v, HA-ketal) and dialyzed against 0.2 M HCl for 2 h. The solution was changed to pH 5.0 with a sodium bicarbonate solution (0.1 M) overnight and then dialyzed against sodium phosphate buffer (0.05 M) pH 5.0 three times before lyophilisation. The degree of substitution was analyzed by ^{1}H NMR in deuterium oxide of the ketone was quantified by comparing the integration of the ketone $-CH_3$ singlet at 2.21 ppm with the *N*-acetamide $-CH_3$ singlet at 2.01 ppm and found to be 40–45% ketone-modified (Fig. S6).

AlexaFluor-647-modified HAK (HAK-647) Ketal-substituted hyaluronan (HA-ketal) (526 mg) was dissolved in 0.1 M MES buffer, pH 6.6 (50 mL) and stirred with DMTMM (0.36 g, 1.31 mmol). After 30 min, AlexaFluor-647 hydrazide (3 mg, dissolved in DMSO at 1 mg mL^{-1}) was added and the reaction was protected from light and stirred overnight. AlexaFluor-647/ketal-substituted hyaluronan (HA-ketal) was dialyzed in 0.1 M NaCl using methyl cellulose dialyzis membrane (12–14 kDa molecular weight cut-off) for 48 h followed by distilled water for 24 h. The ketone was deprotected by dialyzing against 0.2 M HCl for 2 h. The solution was changed to pH 5.0 with a sodium bicarbonate solution (0.1 M) overnight and then dialyzed against sodium phosphate buffer pH 5.0 three times before lyophilisation resulting in a fluffy blue solid. A sample was reconstituted in deuterium oxide for characterization by ^{1}H NMR as described above where the ketone substitution on HA was 40–45%. The substitution of the AlexaFluor-647 was calculated from a standard curve of AlexaFluor-647 hydrazide prepared in 10 mg mL^{-1} HA and the absorbance measured at 650 nm with a NanoDrop instrument. The fluorophore concentration on HAK-647 was calculated to be 149 μmol mg^{-1}. We confirmed that the dialyzis successfully eliminated adsorbed AlexaFluor-647 by measuring the absorbance of a sample from a control reaction conducted with HA-ketal and AlexaFluor-647 hydrazide without DMTMM.

Aldehyde-substituted hyaluronan (HAA) was synthesized as previously reported [51]. Briefly, sodium hyaluronate (1.00 g, 242 kDa) was dissolved in MES buffer (120 mL, 0.1 M in water, pH 5.5) and stirred with DMTMM (0.69 g, 2.5 mmol). After 15 min, aminoacetaldehyde dimethyl acetal (105 mg, 1.0 mmol) was added dropwise and stirred at 60 °C. After 24 h the solution was dialyzed in 0.1 M NaCl using methyl cellulose dialyzis membrane (12–14 kDa molecular weight cut-off) for 48 h followed by distilled water for 24 h. The purified solution was lyophilized to determine acetal substitution (45% acetal-modified). Acetal-substituted hyaluronan (HA-acetal) was dissolved in distilled water and dialyzed against 0.2 M HCl for 48 h. The solution was changed to pH 5.0 with a sodium bicarbonate solution (0.1 M) overnight and then dialyzed against distilled water three times before lyophilisation. Aldehyde-modified hyaluronan (HAA) was characterized as previously reported [52], briefly a sample of HAA (15 mg) was reconstituted in 1 M sodium acetate (pH 5.2) at 10 mg mL^{-1} then *tert*-butyl carbazate (23 mg)

and sodium cyanoborohydride (11 mg) was added and mixed over 24 h. The reaction was dialyzed against 0.1 M NaCl using methyl cellulose dialyzis membrane (12–14 kDa molecular weight cut-off) for 48 h followed by distilled water for 24 h before being lyophilized. A sample of HA-hydrazide (Boc) was reconstituted in deuterium oxide to collect the ^{1}H NMR spectra with 256 scans at 500 MHz the aldehyde substitution was determined using the ratio of integrals corresponding to *tert*-butyl singlet (1.47 ppm) and *N*-acetamide singlet (2.01 ppm) to be 45% aldehyde-modified (Fig. S7).

PEG-tetraoxyamine (PEGOA$_4$) was prepared as previously reported [51]. Briefly, (Boc-aminooxy)acetic acid (0.43 g, 2.3 mmol) and *N,N′*-diisopropylcarbodiimide (DIC) (0.57 mL, 4.6 mmol) were dissolved in 25 mL of dichloromethane (DCM) at 0 °C under nitrogen. After 1 h PEG-tetramine (1.0 g, 5250 Da) was added followed by *N,N*-diisopropylethylamine (1.18 mL, 9.14 mmol), and the reaction was stirred for 48 h at room temperature. DCM was removed in vacuo and the crude was stirred with distilled water and filtered through a 0.22 μm filter to remove the *N,N′*-diisopropylurea byproduct. The filtrate was then dialyzed using methyl cellulose dialyzis membrane (1000 Da molecular weight cut-off) in sodium chloride (0.1 M) for 24 h followed by distilled water for 48 h before being lyophilized. Boc-protected PEG-tetraoxyamine was obtained as a white solid and characterized for substitution by ^{1}H NMR before deprotecting by dialyzis in hydrochloride acid (0.2 M) for 48 h followed by distilled water for 48 h. The dialyzate was lyophilized to give PEG-tetraoxyamine (PEGOA$_4$) was obtained as a white crystalline solid (0.95 g, 46.1% yield). A sample was reconstituted in deuterated chloroform and analyzed by ^{1}H NMR with 512 scans at 500 MHz (Fig. S8). The substitution was confirmed by integrating the signal for the methylene protons (3.6–3.7 ppm) and the singlet for the *tert*-butyl singlet (1.49 ppm) and subsequently the complete deprotection by disappearance of the *tert*-butyl signal and appearance of a singlet (4.3 ppm) representing CO–CH$_2$–O (α to the carbonyl).

2.3. Endotoxin removal and detection

The HA we use is produced by bacteria and rabbit eyes are notoriously sensitive to endotoxins [53], therefore we treated the individual components of our HA-oxime hydrogel with γ phase alumina oxide [54] and achieved an endotoxin concentration of 0.4 ± 0.1 EU mL^{-1} (Fig. S5), which is within an acceptable range of 0.08–0.60 EU mL^{-1} for New Zealand White rabbit eyes [53]. The alumina oxide was separated from the polymers by centrifugation followed by sterile-filtration of the supernatant to provide sterile polymer. To remove endotoxins, each of HAK and HAA were dissolved in ddH$_2$O at 25 mg mL^{-1} and PEGOA$_4$ at 109.5 mg mL^{-1}. Alumina oxide gamma-phase was added at 2 wt% and samples were shaken for 24 h at room temperature. Samples were centrifuged at 2000 rpm to force the alumina to settle. The supernatant was sterile filtered after dilution in ddH$_2$O through a 0.22 μM filter. Samples were then lyophilized. Endotoxin concentrations were determined using a Genscript chromogenic kit by dissolving untreated and alumina treated HAK and HAA at 25 mg mL^{-1} and PEGOA$_4$ at 109.5 mg mL^{-1} in PBS. Standard endotoxin solutions were prepared following the kit protocol and were quantified using a NanoDrop instrument by measuring absorbance at 545 nm (Fig. S9). A linear regression was calculated to determine the concentration of endotoxins in HAK 0.022 ± 0.009 EU mg^{-1}, HAA 0.01 ± 0.01 EU mg^{-1} and PEGOA$_4$ 0.003 ± 0.002 EU mg^{-1}.

2.4. Oxime gel vitreous substitute

Endotoxin reduced HAK and HAA polymers were dissolved at 25 mg mL^{-1} in PBS and incubated at 37 °C for 2 h to dissolve. Endotoxin reduced PEGOA$_4$ was dissolved at 109.5 mg mL^{-1} in 0.1 M phosphate buffer pH 7.4 and sterile filtered. HAK was combined with HAA to give a final polymer concentration of 10.0 mg mL^{-1} and 2.5 mg mL^{-1}, respectively when mixed with 9.48 mg mL^{-1} of PEGOA$_4$. For in vivo studies the polymers were loaded in syringes and combined at a volume ratio of 4:1 (HAK + HAA):PEGOA$_4$, which were mixed through a syringe to syringe connector nine times before being injected.

2.5. Compressive modulus of oxime gel

The compressive moduli of HA-Oxime and HA-Oxime-AF647 hydrogels were measured using a Mach-1 micromechanical system (Biomomentum) connected to a Universal Motion Controller (Newport). Hydrogel samples of 100 μL (0.4 cm^2) were prepared in 16-well chamber slides at 37 °C and equilibrated in PBS overnight before being removed from the chamber slides. Cylindrical samples were placed between two impermeable flat platens and maintained in 50 μL of PBS until they were tested to avoid evaporation (less than 5 min per sample) using a single axis load cell (150 g, ATI Industrial Automation). The height (distance between the two platens) of the samples was measured using an initial force of 0.01 N. To account for any surface defects a uniaxial unconfined compression at 10% strain based on the gel height was applied. Sample compressive modulus was measured by applying a further 10% strain in 5 sequential 2% strain steps. The slope of resultant stress-strain curves for each sample were averaged to calculate the compressive modulus.

2.6. Retinal pigmented epithelial cell compatibility

RPE cells were differentiated from the CA1 human embryonic stem cell line following an established procedure [55,56]. RPE cells were dissociated with trypsin and plated at 5000 cells per well in MEM/F-12, DMEM/F-12 containing 10% fetal bovine serum on 0.4 μm transparent transwells (Corning Life Sciences; catalogue number: C353095) with 300 μL of media beneath the transwell in 24 well plate format. Media above the cells in the transwell was removed and 120 μL of the HA-oxime hydrogel was added directly onto the RPE cells. The plate was maintained at 37 °C for 1 h before an additional 100 μL of media was added above the hydrogel. After 24 h the media above the hydrogel was removed and replaced with media containing 1/250 Hoechst 33342 (nuclei) from a 25 mg mL^{-1} solution in dH$_2$O (Cell Signaling Technology; catalogue number: 4082S), 1/500 calcein AM (live cells) from a 4 mM solution in DMSO (Biotium Inc., catalogue number: 80011-1) and 1/250 ethidium homodimer (dead cells) from a 2 mM solution in DMSO (Biotium Inc., catalogue number: 40014) and incubated for 45 min. The cells were visualized using an Olympus FV1000 confocal microscope and analyzed using Imaris 8 software by Bitplane. Average viability was obtained from three biological replicates.

2.7. Photoreceptor cell compatibility

Photoreceptors were harvested from postnatal day 3–5 *Ccdc136-GFP; Nrl*$^{-/-}$ mice [57], a compound mouse strain in which all rod photoreceptors adopt a cone photoreceptor-like identity (cods) and express GFP. Retinal tissue was dissected in CO$_2$ independent media (Thermo Fisher Scientific, 18045088) and dissociated with papain (Worthington Biochemical Corp., LK003150) following the manufacturer's protocol. Cells were washed in PBS ($Ca^{2+/}Mg^{2+}$-free, Sigma Aldrich, D8537-500 ML) and live cells were counted using 0.4% Trypan blue (Thermo Fisher Scientific, 15250061) as a viability counter stain before being passed through a 40 μm cell strainer (Thermo Fisher Scientific, CLS431750) resuspended in 0.5 mL mL^{-1} DMEM (high glucose, GlutaMAX, pyruvate, Thermo Fisher Scientific, 10569) and 0.5 mL mL^{-1} Nutrient Mixture F12 Ham (Sigma Aldrich, N6658) media containing 10 μL mL^{-1} Sato's supplement, 10 mg mL^{-1} insulin (Sigma Aldrich, I6634) *N*-acetyl-L-cysteine (Sigma Aldrich, A9165) and gentamicin (Thermo Fisher Scientific, 15710) as previously described [58]. Unsorted cells were maintained on ice for less than 1 h before being plated at 10,000 cells per well in media on 0.4 μm transparent transwells (Corning Life Sciences; catalogue number: C353095) with 500 μL of media beneath each transwell in a 24 well plate format. 100 μL of HA-oxime hydrogel was

added per well on the photoreceptor cells once media above the transwell was removed. The plate was maintained at 37 °C for 1 h before an additional 100 μL of media was added above the hydrogel. After 24 h the media above the hydrogel was removed and cells were analyzed by live/dead staining as described earlier. The cells were visualized using an Olympus FV1000 confocal microscope and analyzed using Imaris 8 software by Bitplane. Average viability was obtained from three biological replicates.

2.8. Retinal explant compatibility

Retinas were dissected from postnatal day 4 albino Nrl.gfp mice, Nrl.gfp (transgenic mouse line with post-mitotic rod photoreceptors expressing GFP). They were flat-mounted on transwells (6-well format) and cultured with 1.5 mL serum free media as described [59] on the explant and 2 mL beneath each transwell. 500 μL of the HA-oxime hydrogel was added per explant after 1 d of culture by removing as much media as possible above the explant. After 1 h, 1 mL of media was added on top of the explant. The explants were maintained for 24 h before retinas were dissociated with papain. Viable photoreceptors were quantified using flow cytometry to gate for GFP-labelled cells, annexin V (negative), and 7-aminoactinomycin D (negative) (ThermoFisher Scientific Pacific Blue™ Annexin V/SYTOX™ AADvanced™ Apoptosis kit for flow cytometry; catalogue number: A35136) according to manufacturer's instructions. Average viability was obtained from 3 retinal explants for HA-oxime and 8 retinal explants for media controls.

2.9. New Zealand white rabbit retinal surgeries

Experimental procedures were performed in accordance with the Guide to the Care and Use of Experimental Animals and approved by the Animal Care Committee at the University of Toronto in adherence to the guidelines of the Canadian Council on Animal Care. New Zealand white rabbits (3–4 months) were purchased from Charles River. The surgeries were performed under general anaesthesia with acepromazine 1 mg kg^{-1} prior to induction with isoflurane and intramuscular injection of ketamine 35 mg kg^{-1} and xylazine 5 mg kg^{-1}. Subcutaneous injection of meloxicam 0.2 mg kg^{-1} was administered for pain control and cephalosporin 20 mg kg^{-1} was provided to minimize intraoperative risk of infection and fur surrounding the eye was sterilized with alcohol wipes and iodine. The pupils were dilated using 0.5% tropicamide and 0.5% phenylephrine, and topical anaesthesia with alcaine drops. A surgical microscope (Moller Hi-R 900C) was used to visualize the surgery performed using a Constellation instrument (Alcon) to remove the vitreous with a 23 GA TotalPlus® Vitrectomy Pak while eye pressure was maintained using a balanced saline solution, trochars were carefully placed to avoid touching the lens. The saline was exchanged with gas, and then approximately 1 mL of vitreous gel (HAK, HAA and $PEGOA_4$) or silicone oil (1000-centistoke) was injected into the vitreous cavity. After surgery, the trochars were removed and the areas were sealed with 8-0 vicryl sutures. Animals were treated with Tobradex and received subcutaneous injection of meloxicam 0.2 mg kg^{-1} once a day for at least 2–3 ds following surgery for post-op analgesia. They also received daily application of ophthalmic maxidex to prevent conjunctivitis for at least 2 d, and then as needed. Sham surgeries were performed by placing trochars and infusing saline without a vitrectomy being performed. Intraocular pressure (IOP) was measured using a Tono-Pen tonometer at $t = -1$, 0 and then every 3 d after surgery. The rabbits were sacrificed after 1, 14, 28 or 60 d and both the right and left eyes were harvested from these animals. The eyes were either fixed with Davidson's fix overnight then rinsed with 70% ethanol +0.9% NaCl or covered with 70% ethanol +0.9% NaCl. The eyes were then embedded in paraffin and stained with hematoxylin and eosin (H&E stain) for visualization by microscopy and analysis. Cryosectioned eyes were harvested and immediately flash frozen in 2-methylbutane with dry ice which were stored at −80 °C until sectioning.

2.10. Stability of HA-Oxime gel

After injecting the HA-oxime gel with or without AlexaFluor-647 labelled HAK the remaining hydrogel was collected. The hydrogel was incubated at 37 °C with PBS (1.5 mL mL^{-1} of gel) until the animals were sacrificed. Tissue was dissected to retrieve the hydrogel and weighed. Hydrogels were washed with PBS over 1 h. Hydrogels were speed mixed for 1 min at 3500 rpm to mechanically dissociate the hydrogel. Hyaluronidase was added to the hydrogel from a 10,000 U mL^{-1} stock solution dissolved in PBS to give a final concentration of 1500 U g^{-1} hydrogel. The suspension was incubated overnight at 37 °C and the resulting solutions were pipetted into a clear 96 well plate and quantified using a Tecan instrument with λ_{ex} 640 nm λ_{em} 675 nm. The biodegradation of the HA-oxime hydrogel was modelled using a non-linear regression fit with a one phase exponential decay with least squares fit ($R^2 = 0.982$) with GraphPad Prism 7 and was described by the equation where:

$$\text{Fluorescence} = 100.3\ e^{-0.01585\ *\ \text{Days}}$$

2.11. Rabbit surgeries Dutch belted pigmented rabbits

A total of 3 female Dutch belted rabbits (4 months) were purchased from Envigo. Rabbits were given ketamine 35 mg kg^{-1}, xylazine 5 mg kg^{-1} and induced with acepromazine 1 mg kg^{-1} prior to maintenance with isoflurane 2–3%. Once anesthetized, a subcutaneous injection of meloxicam 0.2 mg kg^{-1} was administered for pain control. Animals were given a subcutaneous injection of cephalosporin 20 mg kg^{-1} to minimize the risk of infection. The fur around the eye was prepared with 2 alternating wipes of alcohol followed by iodine. A sterile eye speculum was inserted, and the pupil was dilated with 0.5% tropicamide, 0.5% phenylephrine, and topical alcaine drops for anaesthesia. Corneal dryness was managed using Tear-Gel and sterile BSS during the vitrectomy procedure carried out with a 23 GA TotalPlus® Vitrectomy Pak while eye pressure was maintained using BSS. The BSS was exchanged with gas, and then approximately 1 mL of either vitreous gel (HA-oxime) or BSS was injected into the vitreous cavity. After surgery, the trochars were removed and the areas were sealed with 8-0 vicryl sutures. Animals were treated with Tobradex and received subcutaneous injection of carprofene 4 mg kg^{-1} twice daily for 2 d following surgery for post-op analgesia. They also received daily application of ophthalmic maxidex to prevent conjunctivitis and given dexamethasone ointment daily for 7 days. Intraocular pressure (IOP) was measured using a Tono-Pen tonometer one week before surgery and every 7 d after surgery. The rabbits were humanely euthanized at 90 d and both the right and left eyes were harvested from these animals. The eyes were either fixed with Davidson's fix overnight then rinsed with 70% ethanol +0.9% NaCl or covered with 70% ethanol +0.9% NaCl.

2.12. Electroretinography

Pupillary dilatation was achieved with topical tropicamide 1% (Mydriacyl) and phenylephrine hydrochloride (Mydfrin; Alcon Canada Inc, Canada). Rabbits were kept in a dark room for 30 min, prepared under dim red illumination, and anesthetized by intramuscular injection of solutions containing ketamine (35 mg kg^{-1}) and xylazine (5 mg kg^{-1}) and maintained by inhalation of 2–3% isoflurane in oxygen with a nose cone. Animals were maintained on a heated pad with intubation and ventilation using intermittent positive pressure. The cornea was treated with a topical anaesthesia, 0.5% proparacaine hydrochloride (Alcaine, Alcon Canada) monopolar ERG Jet contact lens electrodes were positioned on the cornea referenced to a subcutaneous needle electrode placed at the temporal cantus, a subcutaneous electrode inserted behind the ear was used as a ground reference. 0.2% hyaluronan (HYLO Gel Eye

Drops, Candor Vision, Canada) were applied as required to maintain corneal lubrication. Electroretinography (ERG) was performed according to ISCEV standards [60] with additional scotopic stimuli to enable dark-adapted stimulus response series fitting [61]. Recording was performed using Espion E3 electrophysiology system with COLORDOME Ganzfeld stimulator positioned over the rabbits head (Diagnosys LLC, Lowell, MA, USA). Stimuli consisted of brief (<4 ms) flashes of white light. Under scotopic conditions a series of 6 flash intensities evenly spaced from −3 to 1 log cd s m^{-2} were presented. Eyes were then light-adapted using 30 cd m^2 background illumination for 10 min. Under photopic conditions stimuli at 3 cd s m^2 were presented both as individual flashes and as a 30 Hz flicker. All single flash stimuli were repeated at least 3 times with appropriate inter-stimulus intervals to allow for retinal recovery. Repeat responses were averaged and b-wave amplitudes manually measured from the preceding a-wave trough. To avoid diurnal variation in ERG responses, all exams were performed at the same time of the day. Analysis was performed by a clinician blinded to treatment status using R Statistical Analysis software. Dark-adapted intensity response series was fitted to the following function:

$$V = V_{max} I/I + K$$

Where V (μV) is the ERG b-wave amplitude generated in response to flash intensity I (cd s m^{-2}). The derived parameter V_{max} is the asymptotic amplitude of the function, K (cd·s·m^2) is the flash intensity that elicits a response of 50% of Vmax [61].

2.13. Optical coherence tomography

After ERG recording, OCT images of eyes were acquired using Spectralis® instrument by Heidelberg Engineering. Rabbits were maintained under anaesthesia by inhalation of 2–3% isoflurane in oxygen with a nose cone. The eye was manipulated with an atraumatic conjunctival clip to align the globe and elevate the third eyelid. The cornea was hydrated regularly with balanced saline solution (BSS, Alcon Canada) during image acquisition.

3. Results and discussion

3.1. Formulation and physical properties of the HA-oxime vitreous substitute

Hyaluronan was modified with either aldehyde (HAA) or ketone (HAK) and then crosslinked with PEG-tetraoxyamine ($PEGOA_4$) to produce HA-oxime with formulations not previously reported. We evaluated the gelation of the HA-oxime system by varying the ratio of HAK to HAA at constant polymer content (1.25 wt%) with 0.85 wt% $PEGOA_4$ and a molar ratio of 0.5 oxyamine to aldehyde + ketone. Gelation was faster with increased HAA, from 15 ± 3 min to 0.4 ± 0.2 min (Fig. 1B). We selected a subset of the formulations 1.15:0.10, 1.10:0.15 and 1.05:0.20 HAK:HAA, wt%/wt% with gelation rates that were slow enough to mix and handle, and investigated the effect of HAA content on swelling. Hydrogels with 0.10–0.20 wt% HAA were stable during in vitro swelling experiments in balanced saline solution (BSS) used for vitrectomy procedures and remained constant in mass, over 28 d (Fig. 1C). These HA-oxime hydrogels are more stable than higher polymer content PEG-5 wt% hydrazone hydrogels, which degraded by 6 d in vitro [62]. We attribute the high stability of the HA oxime hydrogels due to the nature of the oxime ligation which is more stable to hydrolysis versus the hydrazone ligation [63].

To test injectability of HA-oxime gels, HAK and HAA were mixed with PEGOA4 using a syringe coupler prior to injection. We selected the 1.05:0.20 HAK:HAA, wt%/wt% formulation, which gelled slow enough to be injected but faster than HAK alone, it was stable and injectable by hand based on reported maximum force of 30 N [64] through 23, 25 and 27 gauge needles typically used in surgery (Fig. 1D). Importantly, the mixing and injection processes were both rapid, thereby enabling injection into the vitreous cavity.

We designed our HA-oxime hydrogel to match the properties of the native vitreous and compared these to silicone oil in terms of density, refractive index, transparency and surface tension. The density of the HA-oxime hydrogel is 1.01 ± 0.05 g mL^{-1}, which is similar to the native vitreous (1.01 g mL^{-1}) and higher than that of silicone oil of 0.97 g mL^{-1}. Thus, our HA-oxime hydrogel should fill the vitreous cavity whereas the silicone oil would float. While the issue of a floating vitreous substitute can be overcome with the use of dense intraoperative perfluorocarbon liquids, these are limited by retinal toxicity if left in the eye for more than 2 weeks [5,65]. The refractive indices of the HA-oxime hydrogel (1.356 ± 0.002) and native vitreous (1.334) are comparable due to their high water contents. In contrast, silicone oil has a higher refractive index (1.404), which impacts vision. The surface tension, characterized by contact angle in air (Fig. S1), of HA-oxime is significantly higher 45 ± 5 mN m^{-1} than that of silicone oil 13 ± 3 mN m^{-1} (Fig. 1E), which, given that silicone oil rarely migrates though retinal tears or into the anterior chamber, suggests that our HA-oxime hydrogel will not migrate either.

We wanted to understand how the degradation of the HA-oxime hydrogel impacts transparency, so we studied the process in vitro. An advantage of using an HA hydrogel is that hyaluronidase in the vitreous will degrade it naturally [66]. To mimic accelerated hydrogel biodegradation, we treated samples with hyaluronidase and measured the transparency in gels degraded over 10 d until 32 ± 8% remained (Fig. S2). The transparency of the hydrogel was maintained during degradation, suggesting that vision will not be impacted in vivo during degradation (Fig. 1F). With physical properties that match the native vitreous, which is an improvement upon currently used vitreal substitutes, we sought to further characterize our hydrogel for in vitro cytocompatibility and in vivo biocompatibility.

3.2. In vitro cytocompatibility of HA-oxime hydrogel

To test the cytocompatibility of our HA-oxime hydrogel, we performed in vitro viability assays using a diversity of retinal cells. Human embryonic stem cell-derived RPE maintained 96% viability after 24 h when cultured with HA-oxime, based on calcein AM and ethidium homodimer staining (Fig. S3). Similarly, GFP-labelled cone-like photoreceptors cultured with HA-oxime hydrogel exhibited similar viability as those cells cultured in media after 4 d (Fig. S3). To better understand the interaction with the retina, we cultured HA-oxime hydrogels on mouse retinal explants for 24 h, after which the photoreceptors were dissociated and quantified by flow cytometry (Fig. S4): importantly, there was no significant difference in the number of photoreceptors cultured with or without the HA-oxime hydrogel in terms of cell necrosis (7-aminoactinomycin, 7-AAD) or apoptosis (annexin V) (Fig. 1G), demonstrating that the HA-oxime gel had no deleterious effect on cell viability. These independent in vitro studies confirmed that the hydrogel is cytocompatible with retinal cells, giving us the confidence to test it in vivo.

3.3. In vivo stability of HA-oxime

To monitor stability and degradation, we fluorescently-labelled our HA-oxime hydrogel, and used the depletion of fluorescence as a proxy for degradation for the first time of any vitreous substitute implanted in the eye. We conjugated AlexaFluor-647-hydrazide to carboxylate groups on HAK and confirmed that the mechanical properties of the hydrogel with the fluorescent probe 7 ± 3 kPa were similar to the unlabelled hydrogel 6 ± 3 kPa (Fig. S5). The stability of HA-oxime-AF647 hydrogels was confirmed by comparison to silicone oil after injection into vitrectomized rabbit eyes (Video S1). The vitreous was completely filled by each material, as confirmed by eyes harvested 1 d after injection (Fig. 2A and B). We hypothesized that the hydrogel would gradually disintegrate due to enzymatic degradation of endogenous hyaluronidase and/or by hydrolysis of the oxime bonds. To quantify the stability of HA-oxime-

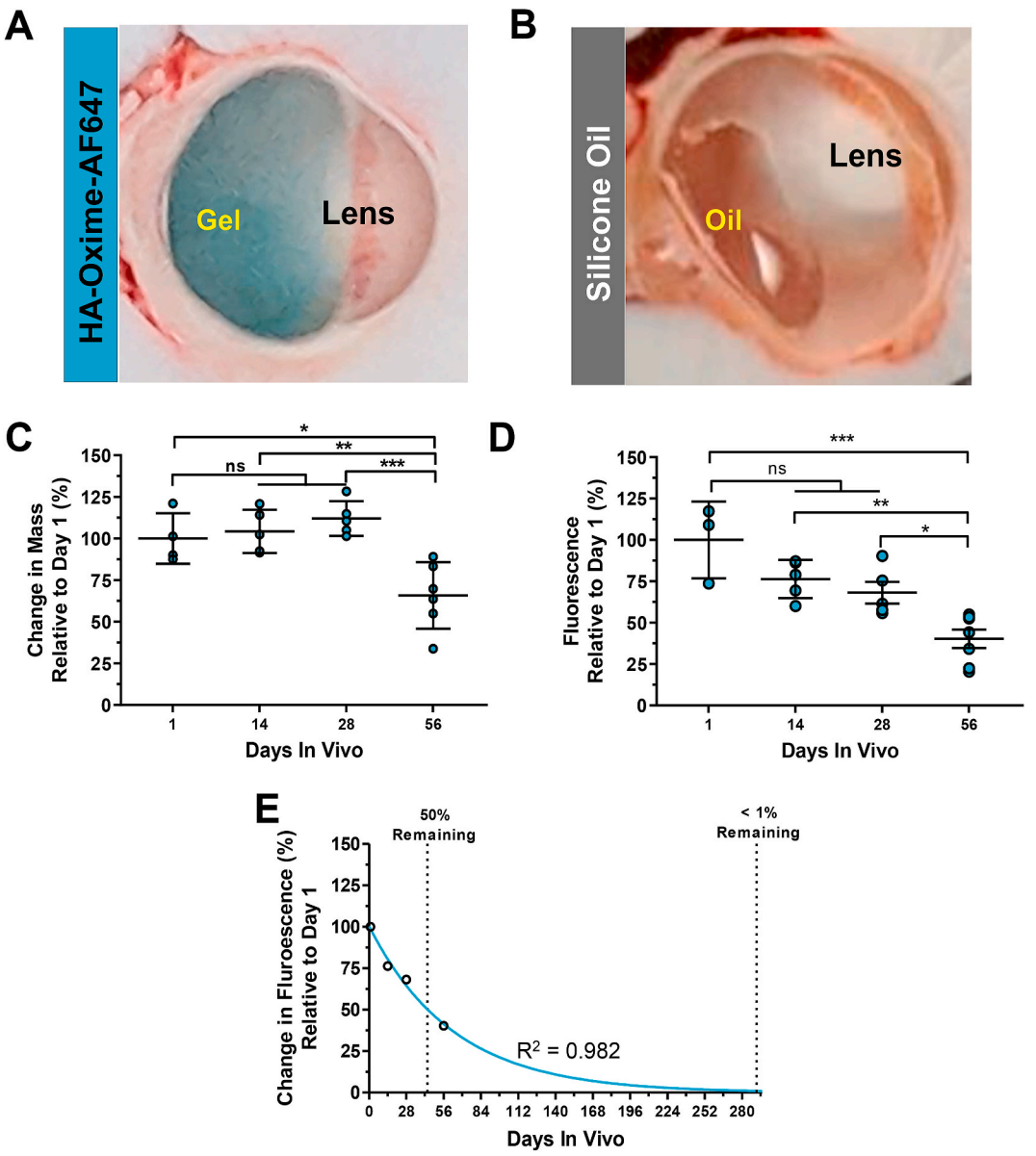

Fig. 2. Stability of HA-oxime hydrogel in rabbit eyes over 56 d. Representative cross-sections of rabbit eyes after vitrectomy and injection of (A) HA-oxime or (B) silicone oil. (C) HA-oxime hydrogels dissected from rabbit eyes were weighed to provide sample mass, which was normalized to day 1 (n = 4 for day 1; n = 5 for day 14 and 28; n = 6 for day 56, mean ± standard deviation, *p < 0.05, **p < 0.01, ***p < 0.001, one-way ANOVA Tukey's post hoc test). (D) Fluorescence of hydrogels dissected from rabbit eyes measured at λ_{ex} = 640 nm and λ_{em} = 675 nm and normalized to day 1 (n = 3 for day 1; n = 5 for day 14 and 28; n = 7 for day 56, mean ± standard deviation, *p < 0.05, **p < 0.01, ***p < 0.001, one-way ANOVA Tukey's post hoc test). (E) Modelled stability of HA-oxime hydrogel in vivo with a half-life of 43 d calculated using a non-linear regression fit with a one phase exponential decay (R^2 = 0.982).

AF647 gels over time, we measured both the mass and fluorescence of the remaining hydrogel. The gel mass was stable until 28 d and then dropped significantly to 60% of its initial mass by 56 d (Fig. 2C). Using the depletion of fluorescence as a measure of HA-oxime stability, the fluorescence of HA-oxime-AF647 decreased steadily to 40 ± 15% of the initial value by day 56 (Fig. 2D). Both techniques demonstrate that the HA-oxime gel degraded by 56 d and each technique has potential drawbacks, thereby necessitating that both techniques were used to gain a greater understanding of material degradation. We acknowledge that the fluorescence loss measured may be greater than that of the mass due to either fluorescent bleaching and/or the gel imbibing proteins or other matter resulting in inaccurate mass measurements. By modelling the in vivo degradation of HA-oxime based on the fluorescence data, we calculated a half-life of 43 d and estimated complete degradation/resorption by 300 d (or 10 months, Fig. 2E). Notwithstanding the different degradation estimates calculated using mass and fluorescence methods over 56 days (65% vs 40%), the HA-oxime hydrogel should last sufficiently long as a vitreous substitute because clinical data has shown that most patients will know the outcome of their retinal detachment surgery (i.e., attached or re-detachment of the retina) within 6 weeks of the procedure [10].

3.4. HA-oxime hydrogel in vivo compatibility

To test the biocompatibility of the HA-oxime hydrogel relative to silicone oil, we examined the retina histologically over time. The rabbit retina remained intact and healthy over the course of 56 d based on histology (Fig. 3A and B). We quantified the number of nuclei (axis oriented from the inner limiting membrane to the Bruch's membrane) present across the ganglion cell layer (GCL), the inner nuclear layer

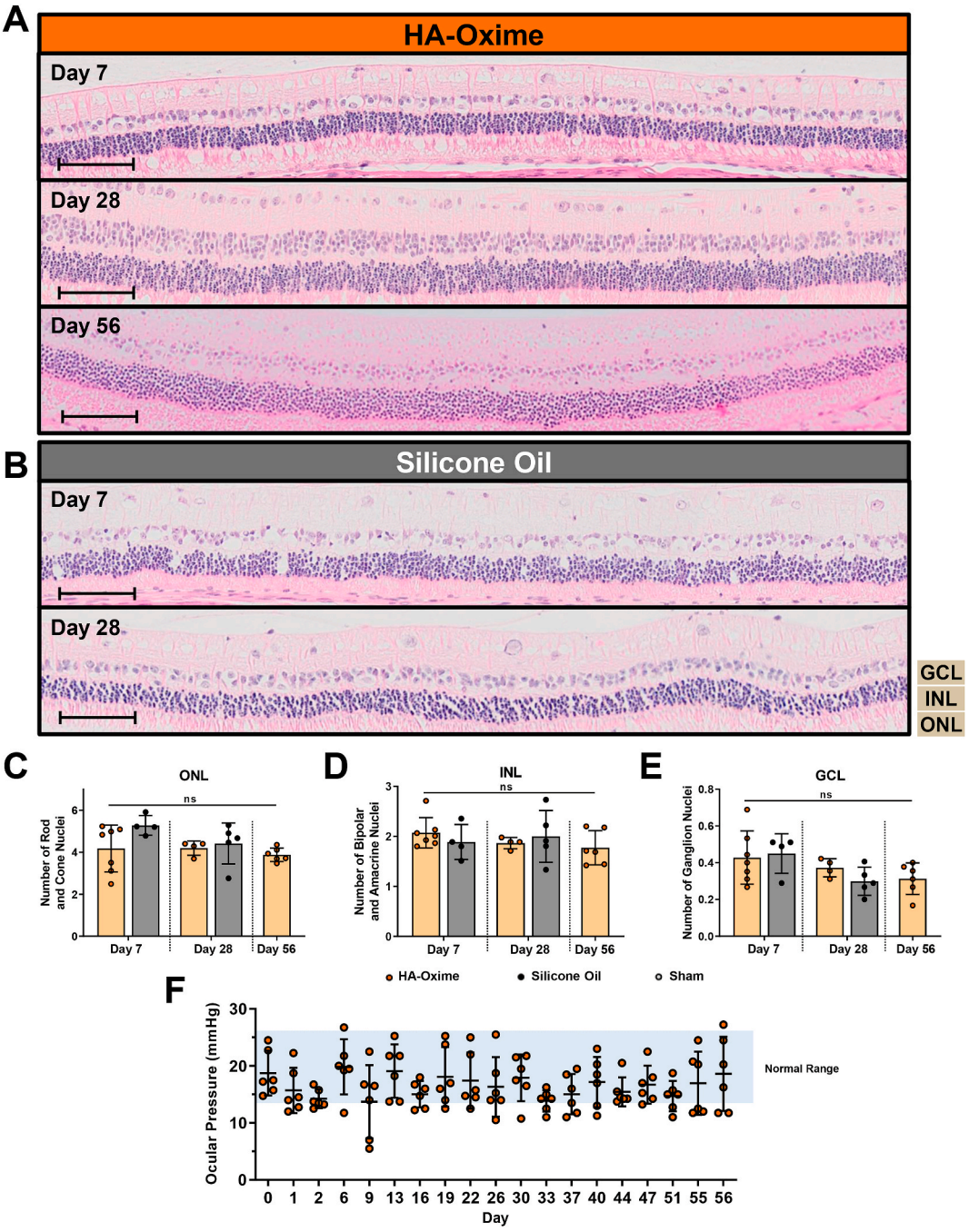

Fig. 3. Histological analyses of the inner and outer nuclear layers of the rabbit retina. (A) Representative hematoxylin and eosin (H&E)-stained retinas of rabbit eyes that had HA-oxime hydrogels therein for 7, 28 and 56 d. (B) Representative hematoxylin and eosin (H&E)-stained retinas of rabbit eyes treated with silicone oil therein for 7 and 28 d. Scale bar represents 100 μm. Quantification of the rabbit (C) outer nuclear layer, (D) inner nuclear layer, and (E) ganglion cell layer retina thickness by number of nuclei counted at 7, 28 and 56 d following injection of HA-oxime or silicone oil ($n = 7$ for HA-oxime day 7; $n = 4$ for silicone oil day 7; $n = 4$ for HA-oxime day 28; $n = 5$ for silicone oil day 28; $n = 6$ for HA-oxime day 56, mean ± standard deviation $p = 0.0382$ (ONL), $p = 0.855$ (INL), and $p = 0.129$ (GCL) one-way ANOVA Tukey's post hoc test). (F) Ocular pressure for rabbits injected with HA-oxime over 56 d ($n = 6$, mean ± standard deviation, $p = 0.780$ for linear regression analysis for non-zero slope).

(INL) which contains containing the bipolar, horizontal, amacrine and Müller glia cells, and the outer nuclear layer (ONL) comprising the rod and cone photoreceptors, at 7, 28 and 56 d. The number of nuclei in the GCL, INL and ONL remained similar across all timepoints (Fig. 3C–E), demonstrating that our new HA-oxime hydrogel is biocompatible. We also confirmed that the vitrectomy procedure was not responsible for any retinal degeneration using a sham surgery which was not statistically different for any of the GCL, INL and ONL thicknesses (Fig. S10). To test whether the hydrogel would swell and exert mechanical force on the retina as it biodegrades, we monitored the ocular pressure using a tonometer (TonoPen). Importantly, the mean ocular pressure remained within the reported normal IOP range for rabbits of 13.50–25.92 mmHg [67] over 56 d (Fig. 3F), thereby demonstrating safety of this hydrogel in vivo. In contrast to the Vitargus hydrogel, which is formed by hydrazone ligation and resulted in ~30% of patients developing elevated IOP, we observed no significant changes in ocular pressure with our HA-oxime hydrogels in New Zealand white rabbit eyes, likely due to the slow hydrolysis rate for oxime linkages versus the faster hydrolysis of

hydrazones [63].

3.5. Retinal function

To better understand the impact of the HA-oxime hydrogel on retinal function, we examined the eyes of dark adapted (DA) Dutch-belted pigmented rabbits by electroretinogram (ERG), optical coherence tomography (OCT) and ocular pressure. Specifically, after vitrectomy, we injected either our HA-oxime hydrogel or BSS each in 3 rabbit eyes. Retina function was measured at baseline and at 4 time points: t = 0, 30,

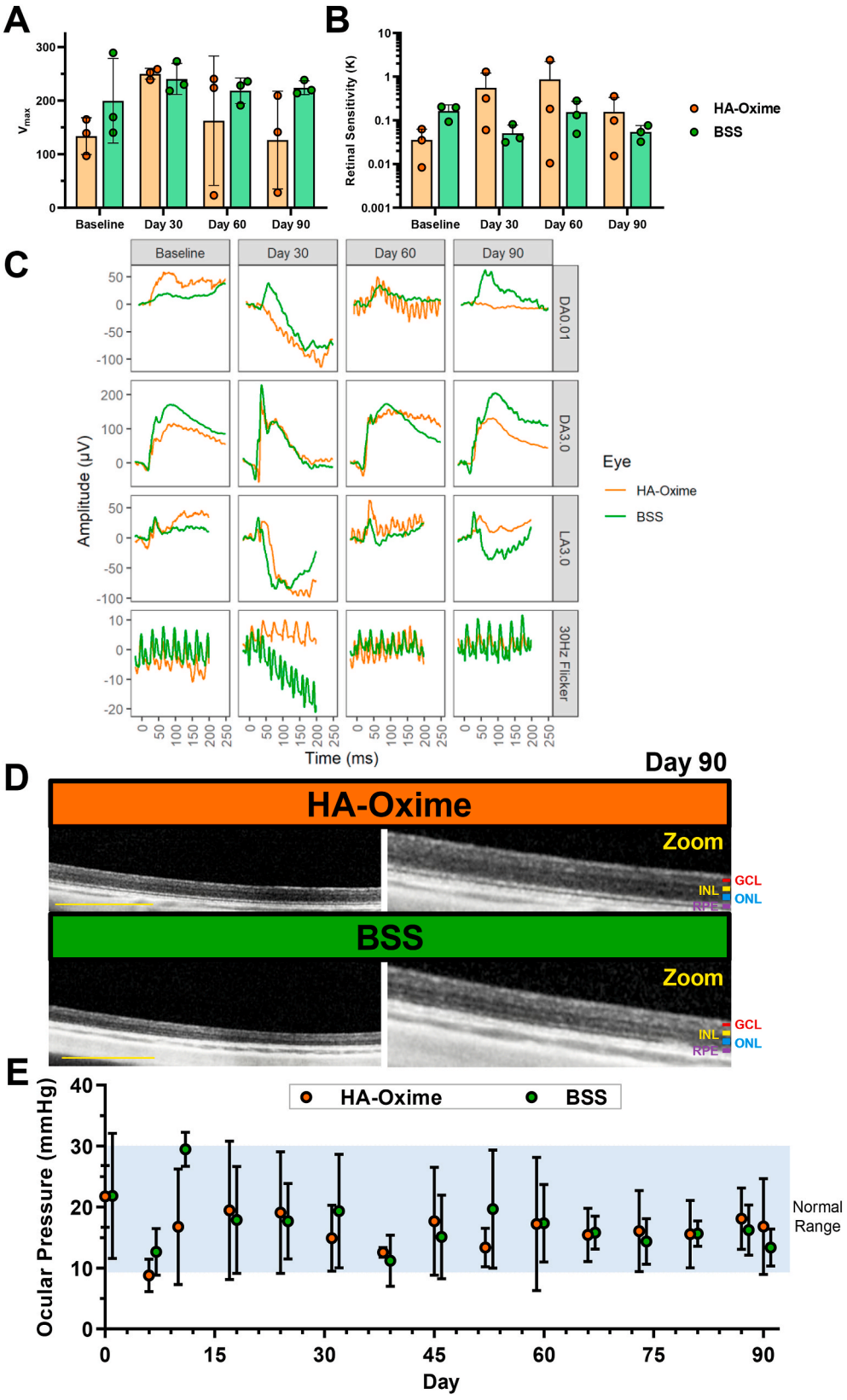

Fig. 4. Analysis of retina function in Dutch-belted pigmented rabbits. (A) Vmax values and (B) retinal sensitivity index (K) calculated from ERG data for eyes injected with HA-oxime or BSS over the course of 90 d (n = 3 eyes per group at each time point, analysis of Vmax results treatment p = 0.157 and time p = 0.199 and interaction p = 0.485; for K results, treatment p = 0.082 and time p = 0.481 and interaction p = 0.608 by two-way ANOVA Bonferroni post hoc test and not statistically significant between treatments for all measurement points). (C) Representative ERG traces for eyes treated with HA-oxime or BSS to evaluate rod isolated (DA 0.01), mixed rod-cone (DA 3.0), cone isolated (LA 3.0), and cone responses (30 Hz flicker). (D) Representative OCT images of the retina after 90 d, scale bar represents 1.0 mm. (E) Ocular pressure with HA-oxime or BSS over 90 d measured by Tono-Pen (n = 3, mean ± standard deviation, p = 0.947 for HA-oxime and p = 0.054 for BSS for linear regression analysis for non-zero slope).

60 and 90 d after injection. After dark-adaptation, we measured the rod isolated, mixed rod-cone, cone isolated, and cone responses to light stimuli by ERG. From these data the Vmax was calculated as an indicator of photoreceptor and retina health. While we acknowledge greater variability with HA-oxime hydrogel injected eyes, based the results of a two-way ANOVA there was no significant change in Vmax values between the treatment groups over the duration of the study, which indicates that the retina remained functional (Fig. 4A). It is possible that the variability is due to a defect in the lens arising naturally or from surgery which can impact ERG values [68]. The index of retinal sensitivity (K), which represents the efficiency of quantal capture by photoreceptors, also remained unchanged in BSS or HA-oxime injected eyes over the 90-d period (Fig. 4B).

The rod photoreceptor function was tested using a dim (0.01 cd) flash under scotopic conditions (DA 0.01) and the resulting traces showed preserved b-wave component. The mixed rod-cone response was captured in the DA 3.0 recordings where the earlier a-wave captures rod and cone hyperpolarizations followed by the b-wave with post-phototransduction to bipolar cells. After light adaptation (LA) the cone isolated response was recorded by LA 3.0 showing evidence of a-wave and b-wave arising from cone photoreceptors. Using the 30 Hz flicker oscillatory potentials arising from cones was measured and shows consistent amplitudes. Traces for the ERG data were consistent with expected findings showing normal retinal responses (Fig. 4C). We confirmed the retina did not become detached with the HA-oxime hydrogel and that the retinal structure was intact, and we could identify the GCL, INL, ONL and RPE layers within HA-oxime and BSS filled eyes using OCT (Fig. 4D). The rabbit eyes were monitored regularly for any signs of redness, inflammation, and corneal or vitreous haze: there were no observed cases of any of these signs. The ocular pressure remained within a normal range over the course of 90 d with either HA-oxime or BSS injected eyes (Fig. 4E). Together these data demonstrate that the HA-oxime hydrogel is safe in terms of retina function.

4. Conclusions

Our new HA-oxime hydrogel matches the properties of the native vitreous in terms of refractive index, density, and transparency. By tuning the ratio of HA-aldehyde to HA-ketone, we were able to control gelation rate and hence injectability. The HA-oxime gel was easily injected in rabbit eyes, filling the vitreous cavity and fulfilling the needs of a vitreous substitute in terms of maintaining normal ocular pressure, resorbing over time and maintaining a healthy functional retina. The key to the success of this hyaluronan hydrogel, where others have failed, is the stable click chemistry, which unlocks the potential for it to be used in a vitreous substitute to treat retinal detachment. While gases and oils work, they have significant disadvantages for patients, requiring eventual replacement with an improved vitreous substitute. In future studies, we will investigate this HA-oxime vitreous substitute in a larger animal model for long-term retina function.

Data availability

All data will be available on Mendeley Data, in a dataset entitled “Original Data: Stable Oxime-crosslinked Hyaluronan-based Hydrogel as a Biomimetic Vitreous Substitute”.

Author contributions

A.E.G.B. designed and executed experiments involving polymer synthesis, rheology, swelling, surface tension, transparency, mechanical testing, in vitro cytocompatibility studies. H.C. performed rheology, characterized hydrogel injectability, produced cryosections of the eyes and analyzed histological sections of the retina. A.E.G.B and H.C. characterized the hydrogel stability in vivo using fluorescently tagged hydrogel. B.B. designed experiments involving mouse retinal explants and provided advice on in vivo experimental design. H.C. and S.I measured intraocular pressure in rabbits and assisted with animal studies. P.Y. and J.W. performed all vitreoretinal surgeries in rabbits and provided advice on experimental design. T.W. provided advice on ERG experimental design, assisted in data collection, and performed the analysis. A.E.G.B, H.C. and M.D. performed ERG experiments and collected OCT images. N.Y.G. performed some vitrectomy procedures in rabbits. M.J.C. provided advice on experimental design. A.O-M. provided culture media, mouse cod cells for in vitro cytocompatibility experiments and provided advice on experimental design. V.A.W., D.v.d.K. R.D., and M.S.S. provided advice on experimental design and M.S.S. supervised this study. A.E.G.B. collected and assembled the data. A.E.G. B and M.S.S. wrote the manuscript. All authors reviewed and commented on the manuscript.

Declaration of competing interest

The authors declare the following financial interests/personal relationships which may be considered as potential competing interests: We wish to draw the attention of the Editor to the following facts which may be considered as potential conflicts of interest and to significant financial contributions to this work. AEGB and MSS acknowledge that a patent has been submitted based on HA-oxime. AEGB, MSS and RD acknowledge that they co-Founded a company to commercialize the vitreous substitute.

Acknowledgements

We are grateful for funding from the Krembil Foundation and initial funding from the Canada First Research Excellence Fund through Medicine by Design at the University of Toronto. Molly Shoichet acknowledges the Canada Research Chairs program for the Tier 1 Chair in Tissue Engineering and Alexander Baker acknowledges the CGSD scholarship from the Natural Sciences and Engineering Research Council of Canada. We acknowledge the Canadian Foundation for Innovation, project number 19119, and the Ontario Research Fund for funding of the Centre for Spectroscopic Investigation of Complex Organic Molecules and Polymers. We thank Hong Cui, Priya Anjea, Peter Poon, Rainerio De Guzman, Anna Pietraszek and Sandra Lafrance for their contributions to the in vivo experiments.

Appendix A. Supplementary data

Supplementary data to this article can be found online at https://doi.org/10.1016/j.biomaterials.2021.120750.

References

[1] B. Lee, M. Litt, G. Buchsbaum, Rheology of the vitreous body: part 3. Concentration of electrolytes, collagen and hyaluronic acid, Biorheology 31 (4) (1994) 339–351, https://doi.org/10.3233/bir-1994-31404.
[2] P.N. Bishop, Structural macromolecules and supramolecular organisation of the vitreous gel, Prog. Retin. 19 (3) (2000) 323–344, https://doi.org/10.1016/S1350-9462(99)00016-6.
[3] T.L. Ponsioen, et al., Collagen distribution in the human vitreoretinal interface, Investig. Ophthalmol. Vis. Sci. 49 (9) (2008) 4089–4095, https://doi.org/10.1167/iovs.07-1456.
[4] H.S. Tan, S.Y. Oberstein, M. Mura, H.M. Bijl, Air versus gas tamponade in retinal detachment surgery, Br. J. Ophthalmol. 97 (1) (2013) 80–82, https://doi.org/10.1136/bjophthalmol-2012-302140.
[5] Q.-C. Li, et al., Effects of perfluorooctane on the retina as a short-term and small amounts remnant in rabbits, Int. J. Ophthalmol. 12 (3) (2019) 381–386, https://doi.org/10.18240/ijo.2019.03.05.
[6] S. Donati, et al., Vitreous substitutes: the present and the future, BioMed Res. Int. 2014 (2014), https://doi.org/10.1155/2014/351804, 351804-351804.
[7] K. Uesugi, et al., A self-assembling peptide gel as a vitreous substitute: a rabbit study, investig, Ophthalmol. Vis. Sci. 58 (10) (2017) 4068–4075, https://doi.org/10.1167/iovs.17-21536.
[8] Z. Liu, et al., Retinal-detachment repair and vitreous-like-body reformation via a thermogelling polymer endotamponade, Nat. Biomed. Eng. 3 (8) (2019) 598–610, https://doi.org/10.1038/s41551-019-0382-7.

[9] K. Hayashi, et al., Fast-forming hydrogel with ultralow polymeric content as an artificial vitreous body, Nat. Biomed. Eng. 1 (3) (2017), 0044, https://doi.org/10.1038/s41551-017-0044.

[10] M.M. Choudhary, M.M. Choudhary, M.U. Saeed, A. Ali, Removal of silicone oil: prognostic factors and incidence of retinal redetachment, Retina 32 (10) (2012) 2034–2038, https://doi.org/10.1097/IAE.0b013e3182562045.

[11] C. Alovisi, C. Panico, U. de Sanctis, C.M. Eandi, Vitreous substitutes: old and new materials in vitreoretinal surgery, 2017, J. Ophthalmol. (2017), https://doi.org/10.1155/2017/3172138, 3172138-3172138.

[12] K. Hayashi, et al., Fast-forming hydrogel with ultralow polymeric content as an artificial vitreous body, Nat. Biomed. Eng. 1 (2017), 0044, https://doi.org/10.1038/s41551-017-0044. https://www.nature.com/articles/s41551-017-0044#supplementary-information.

[13] S. Feng, et al., A novel vitreous substitute of using a foldable capsular vitreous body injected with polyvinylalcohol hydrogel, Sci. Rep. 3 (2013), https://doi.org/10.1038/srep01838, 1838-1838.

[14] J. Liang, et al., Synthesis and characterization of in situ forming anionic hydrogel as vitreous substitutes, J. Biomed. Mater. Res. B Appl. Biomater. 105 (5) (2017) 977–988, https://doi.org/10.1002/jbm.b.33632.

[15] C. Schramm, et al., The cross-linked biopolymer hyaluronic acid as an artificial vitreous substitute, Investig. Ophthalmol. Vis. Sci. 53 (2) (2012) 613–621, https://doi.org/10.1167/iovs.11-7322.

[16] B. Wirostko, B.K. Mann, D.L. Williams, G.D. Prestwich, Ophthalmic uses of a thiol-modified hyaluronan-based hydrogel, Adv. Wound Care 3 (11) (2014) 708–716, https://doi.org/10.1089/wound.2014.0572.

[17] R. Hasslinger, Long-term complications of the MAI hydrogel intrascleral buckling implant, Arch. Ophthalmol. 110 (1) (1992) 12.

[18] M. Roldan-Pallares, et al., MIRAgel: hydrolytic degradation and long-term observations, Arch. Ophthalmol. 125 (4) (2007) 511–514, https://doi.org/10.1001/archopht.125.4.511.

[19] M. Roh, N.G. Lee, J.B. Miller, Complications assoicated with MIRAgel for treatment of retinal detachment, Semin. Ophthalmol. 33 (1) (2018) 89–94, https://doi.org/10.1080/08820538.2017.1353822.

[20] S. Crafoord, S. Andreasson, F. Ghosh, Experimental vitreous tamponade using polyalkylimide hydrogel, Graefes Arch. Clin. Exp. Ophthalmol. 249 (8) (2011) 1167–1174, https://doi.org/10.1007/s00417-011-1652-6.

[21] M. Machida, M.I. Machida, Y. Kanaoka, Hydrolysis of N-substituted maleimides: stability of fluorescence thiol reagents in aqueous media, Chem. Pharm. Bull. 25 (10) (1977) 2739–2743.

[22] N. Hisano, et al., Kinetic analyses of disulfide formation between thiol groups attached to linear poly(acrylamide), J. Polym. Sci. Polym. Chem. 49 (3) (2011) 671–679, https://doi.org/10.1002/pola.24478.

[23] J. Stefater, Anthony III, Stryjewski, P. Tomasz, Methods and Polymer Compositions for Treating Retinal Detachment and Other Ocular Disorders, 2017, WO2018013819A1.

[24] S. Maruoka, et al., Biocompatibility of polyvinylalcohol gel as a vitreous substitute, Curr. Eye Res. 31 (7–8) (2006) 599–606, https://doi.org/10.1080/02713680600813854.

[25] M. Nakagawa, M. Tanaka, T. Miyata, Evaluation of collagen gel and hyaluronic acid as vitreous substitutes, Ophthalmic Res. 29 (6) (1997) 409–420.

[26] X. Su, et al., Recent progress in using biomaterials as vitreous substitutes, Biomacromolecules 16 (10) (2015) 3093–3102, https://doi.org/10.1021/acs.biomac.5b01091.

[27] S. Schnichels, et al., Efficacy of two different thiol-modified crosslinked hyaluronate formulations as vitreous replacement compared to silicone oil in a model of retinal detachment, PloS One 12 (3) (2017), e0172895, https://doi.org/10.1371/journal.pone.0172895.

[28] C. Schramm, et al., The cross-linked biopolymer hyaluronic acid as an artificial vitreous substitute, Invest. Ophthalmol. Vis. Sci. 53 (2) (2012) 613–621, https://doi.org/10.1167/iovs.11-7322.

[29] R.C. Pruett, G.A. Calabria, C.L. Schepens, Collagen vitreous substitute: I. Experimental study, Arch. Ophthalmol. 88 (5) (1972) 540–543, https://doi.org/10.1001/archopht.1972.01000030542015.

[30] J.L. Denlinger, E.A. Balazs, Replacement of the liquid vitreus with sodium hyaluronate in monkeys : I. Short-term evaluation, Exp. Eye Res. 31 (1) (1980) 81–99, https://doi.org/10.1016/0014-4835(80)90092-5.

[31] H. Barth, S. Crafoord, S. Andréasson, F. Ghosh, A cross-linked hyaluronic acid hydrogel (Healaflow®) as a novel vitreous substitute, Graefes Arch. Clin. Exp. Ophthalmol. 254 (4) (2016) 697–703, https://doi.org/10.1007/s00417-015-3256-z.

[32] R.C. Pruett, C.L. Schepens, D.A. Swann, Hyaluronic acid vitreous substitute. A six-year clinical evaluation, Arch. Ophthalmol. 97 (12) (1979) 2325–2330, https://doi.org/10.1001/archopht.1979.01020020541006.

[33] K. Januschowski, et al., Ex vivo biophysical characterization of a hydrogel-based artificial vitreous substitute, PloS One 14 (1) (2019), e0209217, https://doi.org/10.1371/journal.pone.0209217.

[34] W.Y. Su, et al., An injectable oxidated hyaluronic acid/adipic acid dihydrazide hydrogel as a vitreous substitute, J. Biomater. Sci. Polym. Ed. 22 (13) (2011) 1777–1797, https://doi.org/10.1163/092050610x522729.

[35] A. Chang, Vitreous Substitutes Following Vitrectomy Surgery, American Academy of Ophthalmology, San Francisco, California, 2019.

[36] J.M. Skeie, C.N. Roybal, V.B. Mahajan, Proteomic insight into the molecular function of the vitreous, PloS One 10 (5) (2015), e0127567, https://doi.org/10.1371/journal.pone.0127567.

[37] J. Collins, Z. Xiao, M. Müllner, L.A. Connal, The emergence of oxime click chemistry and its utility in polymer science, Polym. Chem. 7 (23) (2016) 3812–3826, https://doi.org/10.1039/C6PY00635C.

[38] J.G. Hardy, P. Lin, C.E. Schmidt, Biodegradable hydrogels composed of oxime crosslinked poly(ethylene glycol), hyaluronic acid and collagen: a tunable platform for soft tissue engineering, J. Biomater. Sci. Polym. Ed. 26 (3) (2015) 143–161, https://doi.org/10.1080/09205063.2014.975393.

[39] S. Wang, et al., Influence of ions to modulate hydrazone and oxime reaction kinetics to obtain dynamically cross-linked hyaluronic acid hydrogels, Polym. Chem. 10 (31) (2019) 4322–4327, https://doi.org/10.1039/c9py00862d.

[40] D. Larsen, et al., Exceptionally rapid oxime and hydrazone formation promoted by catalytic amine buffers with low toxicity, Chem. Sci. 9 (23) (2018) 5252–5259, https://doi.org/10.1039/C8SC01082J.

[41] M. Wendeler, et al., Enhanced catalysis of oxime-based bioconjugations by substituted anilines, Bioconjugate Chem. 25 (1) (2014) 93–101, https://doi.org/10.1021/bc400380f.

[42] M.R. Lalonde, M.E. Kelly, S. Barnes, Calcium-activated chloride channels in the retina, Channels 2 (4) (2008) 252–260, https://doi.org/10.4161/chan.2.4.6704.

[43] S. Barnes, V. Merchant, F. Mahmud, Modulation of transmission gain by protons at the photoreceptor output synapse, Proc. Natl. Acad. Sci. U. S. A. 90 (21) (1993) 10081–10085, https://doi.org/10.1073/pnas.90.21.10081.

[44] E.P. Meyertholen, M.J. Wilson, S.E. Ostroy, The effects of hepes, bicarbonate and calcium on the cGMP content of vertebrate rod photoreceptors and the isolated electrophysiological effects of cGMP and calcium, Vis. Res. 26 (4) (1986) 521–533, https://doi.org/10.1016/0042-6989(86)90001-5.

[45] M.J. Ogidigben, D.E. Potter, Central imidazoline (I(1)) receptors modulate aqueous hydrodynamics, Curr. Eye Res. 22 (5) (2001) 358–366, https://doi.org/10.1076/ceyr.22.5.358.5492.

[46] J.D. Brown, R.F. Brubaker, A study of the relation between intraocular pressure and aqueous humor flow in the pigment dispersion syndrome, Ophthalmology 96 (10) (1989) 1468–1470, https://doi.org/10.1016/s0161-6420(89)32703-5.

[47] S.D. Walker, R.F. Brubaker, S. Nagataki, Hypotony and aqueous humor dynamics in myotonic dystrophy, Investig. Ophthalmol. Vis. Sci. 22 (6) (1982) 744–751.

[48] M. Shah, et al., Translational preclinical pharmacologic disease models for ophthalmic drug development, Pharm. Res. (N. Y.) 36 (4) (2019) 58, https://doi.org/10.1007/s11095-019-2588-5.

[49] R.S. Leang, et al., Preclinical safety evaluation of ophthalmic viscosurgical devices in rabbits and a novel mini-pig model, Ophthalmol. Ther. 8 (1) (2019) 101–114, https://doi.org/10.1007/s40123-019-0167-9.

[50] A.E.G. Baker, et al., Benchmarking to the gold standard: hyaluronan-oxime hydrogels recapitulate xenograft models with in vitro breast cancer spheroid culture, Adv. Mater. 31 (36) (2019) 1901166, https://doi.org/10.1002/adma.201901166.

[51] A.E.G. Baker, et al., Benchmarking to the gold standard: hyaluronan-oxime hydrogels recapitulate xenograft models with in vitro breast cancer spheroid culture, Adv. Mater. (2019) 1901166, https://doi.org/10.1002/adma.201901166, 0(0).

[52] A.E.G. Baker, R.Y. Tam, M.S. Shoichet, Independently tuning the biochemical and mechanical properties of 3D hyaluronan-based hydrogels with oxime and Diels-Alder chemistry to culture breast cancer spheroids, Biomacromolecules 18 (12) (2017) 4373–4384, https://doi.org/10.1021/acs.biomac.7b01422.

[53] S.Y. Buchen, D. Calogero, G. Hilmantel, M.B. Eydelman, Rabbit ocular reactivity to bacterial endotoxin contained in aqueous solution and ophthalmic viscosurgical devices, Ophthalmology 119 (7) (2012) e4–e10, https://doi.org/10.1016/j.ophtha.2012.04.006.

[54] S. Choi, et al., Purification and biocompatibility of fermented hyaluronic acid for its applications to biomaterials, Biomater. Res. 18 (1) (2014) 6, https://doi.org/10.1186/2055-7124-18-6.

[55] O. Adewumi, et al., Characterization of human embryonic stem cell lines by the International Stem Cell Initiative, Nat. Biotechnol. 25 (7) (2007) 803–816, https://doi.org/10.1038/nbt1318.

[56] J. Parker, N. Mitrousis, M.S. Shoichet, Hydrogel for simultaneous tunable growth factor delivery and enhanced viability of encapsulated cells in vitro, Biomacromolecules 17 (2) (2016) 476–484, https://doi.org/10.1021/acs.biomac.5b01366.

[57] S. Smiley, et al., Establishment of a cone photoreceptor transplantation platform based on a novel cone-GFP reporter mouse line, Sci. Rep. 6 (1) (2016) 22867, https://doi.org/10.1038/srep22867.

[58] E.L.S. Tsai, et al., Modeling of photoreceptor donor-host interaction following transplantation reveals a role for crx, müller glia, and rho/ROCK signaling in neurite outgrowth, Stem Cell. 37 (4) (2019) 529–541, https://doi.org/10.1002/stem.2985.

[59] B.L.K. Coles, D.J. Horsford, R.R. McInnes, D. van der Kooy, Loss of retinal progenitor cells leads to an increase in the retinal stem cell population in vivo, Eur. J. Neurosci. 23 (1) (2006) 75–82, https://doi.org/10.1111/j.1460-9568.2005.04537.x.

[60] D.L. McCulloch, et al., ISCEV Standard for full-field clinical electroretinography (2015 update), Doc. Ophthalmol. 130 (1) (2015) 1–12, https://doi.org/10.1007/s10633-014-9473-7.

[61] M.A. Johnson, B.G. Jeffrey, A.M.V. Messias, A.G. Robson, ISCEV extended protocol for the stimulus-response series for the dark-adapted full-field ERG b-wave, Doc. Ophthalmol. 138 (3) (2019) 217–227, https://doi.org/10.1007/s10633-019-09687-6.

[62] N. Boehnke, et al., Imine hydrogels with tunable degradability for tissue engineering, Biomacromolecules 16 (7) (2015) 2101–2108, https://doi.org/10.1021/acs.biomac.5b00519.

[63] J. Kalia, R.T. Raines, Hydrolytic stability of hydrazones and oximes, Angew. Chem., Int. Ed. Engl. 47 (39) (2008) 7523–7526, https://doi.org/10.1002/anie.200802651.
[64] T.E. Robinson, et al., Filling the gap: a correlation between objective and subjective measures of injectability, Adv Healthc Mater 9 (5) (2020), e1901521, https://doi.org/10.1002/adhm.201901521.
[65] U. Stolba, K. Krepler, M. Velikay-Parel, S. Binder, The effect of specific gravity of perfluorocarbon liquid on the retina after experimental vitreous substitution, Graefes Arch. Clin. Exp. Ophthalmol. 242 (11) (2004) 931–936, https://doi.org/10.1007/s00417-004-0916-9.
[66] D.M. Schwartz, et al., Human vitreous hyaluronidase: isolation and characterization, Curr. Eye Res. 15 (12) (1996) 1156–1162, https://doi.org/10.3109/02713689608995150.
[67] M.A. Zouache, I. Eames, A. Samsudin, Allometry and scaling of the intraocular pressure and aqueous humour flow rate in vertebrate eyes, PloS One 11 (3) (2016), e0151490, https://doi.org/10.1371/journal.pone.0151490.
[68] R.F. Sanchez, et al., Rabbits with naturally occurring cataracts referred for phacoemulsification and intraocular lens implantation: a preliminary study of 12 cases, Vet. Ophthalmol. 21 (4) (2018) 399–412, https://doi.org/10.1111/vop.12525.